Journal of Advanced Research in Fluid Mechanics and Thermal Sciences

Journal homepage:
https://semarakilmu.com.my/journals/index.php/fluid_mechanics_thermal_sciences/index
ISSN: 2289-7879

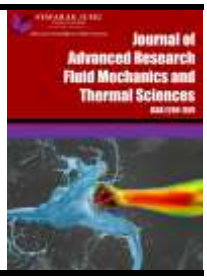

Porous Lining and Inclination Effects on Peristaltic Flow in a Non-Uniform Tube

Revanasidda Metri[1], Gurunath Sankad[1,*], Sharanabasayya Gurushantanavar[2]

[1] Department of Mathematics, B.L.D.E.A's V. P. Dr P.G.Halakatti College of Engineering and Technology, Vijayapur (586103), Karnataka, India
[2] Department of Mathematics, Basaveshwar Engineering College, Bagalkote (587103), Karnataka, India

ARTICLE INFO

Article history:
Received 7 April 2024
Received in revised form 9 July 2024
Accepted 18 July 2024
Available online 15 August 2024

Keywords:
Peristalsis; porous tube; pressure drop; slip parameter

ABSTRACT

The consequences of varying pressure drop on a Herschel-Bulkley fluid as it flows through two-dimensional non-uniform porous tube have been explored. The governing equations of the model were solved analytically under long wavelength and low Reynolds number to determine the behavior of the fluid within the given conditions. Exact solutions are derived for the velocity field, stream functions, and pressure gradient. The observations disclose that an increase in the porous thickening of the wall enhances the pressure rise. The rise in Darcy's numbers reduces the pressure rise. This suggests an inverse relationship between Darcy's number and pressure difference. Also, the impact of various parameters involved in the solutions is presented graphically. The article concludes with a discussion on the trapping phenomena for Herschel-Bulkley fluid.

1. Introduction

Peristalsis is a molecular machine found in biological systems that facilitates in the movement of biological fluids. The propulsion of surrounding warms, the passage of lymph in the lymphatic pots, and the vasomotion of secondary blood vessels such as capillary artery, capillary veins, and vessels involved in the rippling signal are all examples of how this fluid passage device has traditionally been a significant consideration in current periods in to production and biological knowledge. Numerous studies use the peristaltic flow of non-Newtonian fluids through pipes to gauge how well efficient fluids operate in terms of flow.

In order to transport fluid upwards or downwards, peristaltic pumps involve flexible tubing that passes over a roller wheel (also known as rollers or shoes) that is positioned in the pump head. By doing this, the tube is confined, increasing the low-pressure volume. This results in the creation of a vacuum, which draws the liquid into the tube. Fluid packets are formed when they pass through the pump head. The flow rate is determined by the size of the packets and the rotational speed of the rollers.

* *Corresponding author.*
E-mail address: math.gurunath@bldeacet.ac.in

https://doi.org/10.37934/arfmts.120.1.3556

Latham [1] was the creative detective who considered fluid wave in a peristaltic drive. Gupta and Seshadri [2] have discussed the pressure drop completed the pipe measurement at any certain movement rate, and largeness ratio is found to be abundantly less related to that in unchanging geometry. Misra and Pandey [3] studied Peristaltic passage of plasma in small pots. Srinivasacharya *et al.,* [4] conferred peristaltic propelling of a micropolar liquid in a tube. Rani and Sarojamma [5] discussed the rippling transport of a Casson watery in an irregular channel. Rao and Mishra [6] have analyzed Peristalsis the whole thing as a drive compared to a greater compression increase for a trim deepening liquid, and the contradictory occurs for a trim retreating liquid, associated with Newtonian liquid. Reddy [7] investigated how the magnitude of the surrounding bolus increases with a growing speed error limit.

The non-Newtonian fluid has persistent viscosity and self-governing stress. In non-Newtonian fluids, thicknesses can modify when under strength to either extra liquid or additional solid. Catch-up, for example, develops runnier when surprised and is thus a non-Newtonian fluid. Various salty resolutions and melted polymers exhibit persistent stickiness independent of strain resolutions by way of numerous commonly derived substances such as life blood, honey, toothpaste, amylum suspensions, shade, melted fat, and shampoo.

The usage of non-Newtonian fluids has become practically an important need for manufacturing, buildings, and health science. Therefore, the study of different technical machinery with non-Newtonian liquids has similarly expanded. Nadeem and Akbar [8] discussed the liquid movement in the tendency edge of position moving with the speed of the rippling movement. Maiti and Misra [9] investigated rippling motion of plasma in the micro-circulatory structure by considering the non-uniform geometry of the arterioles and capillary vein. Sankad and Patil [10] discussed the consequences of permeability following the peristaltic propelling of a non-Newtonian liquid in a canal.

Herschel-Bulkley fluid is a non-Newtonian fluid considered to be the more general fluid, providing more exact outcomes than further methods of non-Newtonian liquids, in which the straining experienced by the liquid is related to the pressure in a difficult, non-linear way. To study lifeblood, preferably the Herschel Bulkley fluid representative is suggested for its combined performance with blood and its resistance to reduction into the Bingham, Newtonian and Power law models.

Vajravelu *et al.,* [11-13] discussed Peristaltic pumping of a Herschel Bulkley Fluid in a channel or tube and later investigated peristaltic pumping of a Herschel–Bulkley fluid in contact with a Newtonian fluid. Selvi and Srinivas [14] have analyzed the fluctuation of Herschel-Bulkley liquid in a non-uniform pipe through rippling, and resistance declines as the liquid performance index rises.

In uniform pipeline, the cross section of each channel of the tube remains unaffected and all particles grows laterally along the situation axis through endless speediness. A non-uniform movement is one in which speed is not continuous at a given Instant. A flow in which the amount of fluid elegant per second is non-persistent is called unsteady movement. Unsteady flow may also include periodic motion such as that of waves on beaches.

Pandey and Tripathi [15] investigated the rippling motion of a viscous liquid below the impact of a magnetic ground over a pipe of fixed distance in a dimensionless system. Takagi and Balmforth [16] investigated the numerical resolutions for sporadic tendency trains and solitary waves that are obtainable laterally through asymptotic resolutions at both minor and huge forcing amplitudes. Prasad *et al.,* [17] discussed that the temperature outline has a reverse behavior compared to nanoparticle singularities, and the size of the surrounding bolus in multi sinusoidal tendency is minor as associated with the sinusoidal movement. Sankad and Patil [18] calculated the pumping influences

of dissimilar parameters taking place in the flow of Herschel Bulkley liquid in a non-uniform canal with a permeable lining.

Kavitha *et al.,* [19] analyzed the difference in time-averaged instability with pressure increase, the boundary shape is found, and the variation of the boundary shape gives escalation to the solvent peripheral area with growing Jeffrey fluid constraint. Vaidya [20] calculated that the effect of Jeffery constraint and angle of inclination improves the stream rate, while the effects of flexible limitations, outlet flexible area, and breadth ratio raise the flow rate while inlet flexible constraint reduces the stream rate. Gudekote and Choudhari [21] exhibited the peristaltic motion of blood in the human circulatory system. Devaki *et al.,* [22] have discussed the impact of various parameters on peristaltic transport of a Casson fluid in a conduit. Vaidya *et al.,* [23] analyzed Peristaltic flow of non-Newtonian fluid through an inclined nonlinear tube: application to chyme transport in the gastrointestinal tract. Ramachandran *et al.,* [24] have calculated the peristaltic-ciliary flow of a Casson fluid through an inclined tube. Devakar *et al.,* [25] discussed the effect of different parameters of wall and fluid properties on the velocity and stream function. The rheology of the peristaltic flow of Couple stress fluid in an inclined tube has been examined by Abbas *et al.,* [26]. The influence of thermal skip and inclined magnetic field on peristaltic transport of Jeffrey fluid with silver nanoparticles in the eccentric annulus was analyzed by Kotnurkar and Talawar [27]. Moatimid *et al.,* [28] have analyzed the fluctuation of Rabinowitsch nanofluid with moving microorganisms through peristalsis. Ali *et al.,* [29] proposed a novel dynamic meshing technique for peristaltic pumping problems, and this numerical technique is based on the finite volume method. Abuiyada *et al.,* [30] investigated the influence of the chemical reaction and activation energy on MHD peristaltic flow of Jeffery nanofluids in an inclined symmetric channel through a porous medium.

The text discusses the significance of peristalsis in manufacturing, building, and health sciences. A more detailed exploration of interdisciplinary applications, potential innovations, and technological peristaltic research could lead to beneficial advancements. In summary, peristalsis and the study of non-Newtonian fluids, especially the Herschel-Bulkley fluid, have widespread applications in diverse fields, with researchers exploring various aspects and parameters to enhance our understanding of fluid dynamics. The provided text extensively covers research on peristalsis and the transport of non-Newtonian fluids through various channels and tubes, especially focusing on the Herschel-Bulkley fluid. However, there are certain research gaps, especially in non-uniform geometries with porous linings. Accordingly, this research focuses on examining the effects of porous lining and tube inclination on the peristaltic movement of Herschel-Bulkley fluid. In the end, the impact of the outcome of an unstable pressure drop on Herschel-Bulkley fluid in an inclined porous tube was studied and examined comprehensively.

2. Fundamental Equations

The fundamental equations governing the flow of an incompressible fluid are [12]

$$\text{div}\, V = 0, \tag{1}$$

$$\text{div}\, \sigma + \rho f = \rho \frac{dV}{dt}, \tag{2}$$

where V is the velocity, ρ fluid density of the fluid, f is the body force per unit mass and $\frac{d}{dt}$ the material derivative. The Cauchy's stress σ is given by

$$\sigma = -PI + T, \tag{3}$$

$$T = 2\mu D + S, \tag{4}$$

$$S = 2\eta D. \tag{5}$$

In which D is the symmetric part of the velocity gradient, which is

$$D = \tfrac{1}{2}(L + L^T),\ L = \text{grad}\, V. \tag{6}$$

Also, μ and η are viscosities, while PI stands for the undetermined portion of stress caused by the incompressibility restriction.

The fluid model known as Hershel-Bulkley combines power law and Bingham effects. The stiff material behaves like a highly viscous fluid with viscosity μ_0 at low strain rates $\left(\dot{\gamma} < \frac{\tau_0}{\mu}\right)$. A power law describes the fluid behavior as τ_0 passes the threshold of increased strain rate [12].

Once the yield stress has been reached, the Herschel-Bulkley model's constitutive equation can be expressed as follows

$$\tau = \mu\dot{\gamma}^n + \tau_0, \quad \text{for} \quad \tau \geq \tau_0$$

$$\dot{\gamma} = 0, \qquad \text{for} \quad \tau < \tau_0$$

where $\tau -$ is the shear stress, τ_0- the yield stress, $\dot{\gamma}$- the shear stress and *n* the flow index.

3. Mathematical Construction

Deliberate the peristaltic transference of a Herschel-Bulkley fluid in a tending, non-uniform pipe of radius a (Figure 1). The tube is tending at an angle β with the horizontal. Deliberate the cylindrical organizes scheme in (r, z, t). Herschel-Bulkley liquid movement inside a non-uniform circular tube is considered peristaltic wave through the coordinate system(r, z, t). The lifeblood movement is demonstrated to be laminar, incompressible, two-dimensional, full-developed, and axisymmetric and demonstrates the peristaltic motion of Herschel-Bulkley liquid in a flexible tube of radius a_0. The area between $r = 0$ and $r = r_0$ named plug flow region, where $|\tau_{rz}| \leq \tau_0$. in the region between $r = r_0$ and $r = a(z, t)$, and we have $|\tau_{rz}| \geq \tau_0$.

The deformation of wall due to the transmission of sinusoidal waves is signified as

$$h(z, t) = a_0 + b \sin\frac{2\pi}{\lambda}(z - ct), \tag{7}$$

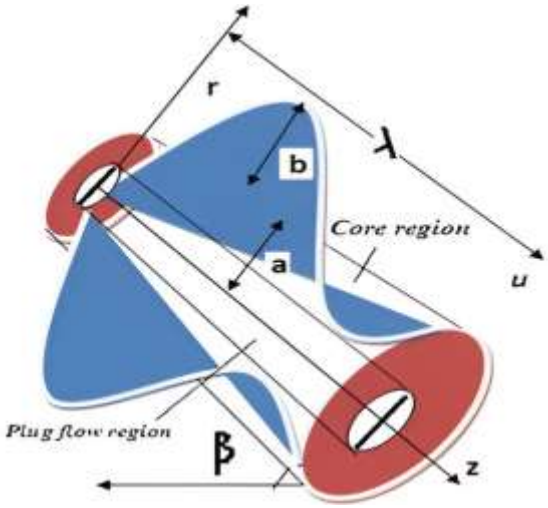

Fig. 1. Geometry of the problem

where $a_0 = a + dz$, a_0: the average radius of the tube; λ: the wavelength; b: the amplitude of the movement and *c:* the movement speediness.

We make the assumptions that the pressure differentials between the tube's ends are constant and that the tube length is an integral multiple of the wavelength λ. Moving with velocity *c* away from the fixed frame $(R, \emptyset, Z)$, the flow becomes unsteady in the laboratory frame $(R, \emptyset, Z)$ and steady in the wave frame (r, θ, z). The change between these two frames is described as

$$r = R, \quad z = Z - ct, \quad \boldsymbol{\psi} = \boldsymbol{\psi} - \frac{\boldsymbol{R^2}}{\boldsymbol{2}}, \quad \boldsymbol{p(Z,t)} = \boldsymbol{P(z)}, \tag{8}$$

where *p* and *P* represent pressures in the wave and fixed frames of reference, respectively, and $\boldsymbol{\psi}$ and $\boldsymbol{\psi}$ are stream functions. Assuming a long wavelength approximation, the pressure *p* stays constant at any axial station of the tube. Making use of the subsequent non-dimensional quantities,

$$\bar{r} = \frac{r}{a_0},\ \bar{z} = \frac{z}{\lambda},\ \bar{t} = \frac{ct}{\lambda},\ l = \frac{b}{a},\ \bar{F} = \frac{F}{\lambda \mu c},\ \psi = \frac{\psi}{\pi a^2 c},\ \bar{u} = -\frac{1}{r}\frac{\partial \psi}{\partial r},\ \bar{w} = \frac{1}{r}\frac{\partial \psi}{\partial r},\ \bar{q} = \frac{q}{\pi {a_0}^2 c},\ Da = \frac{k}{a^2},\ \bar{Q} = \frac{Q}{\pi {a_0}^2 c},\ \bar{a} = \frac{a}{a_0},\ \bar{\tau}_0 = \frac{\tau_0}{\mu\,(U/a_0)^n},\ \bar{\tau}_{rz} = \frac{\tau_{rz}}{\mu\,(U/a_0)^n},\ \bar{r}_0 = \frac{r_0}{a_0},\ \bar{p} = \frac{{a_0}^{n+1}}{\lambda \mu c^n} P, \tag{9}$$

where $\bar{u}$, $\bar{w}$ are the radial and axial velocities in the wave border and $\bar{\tau}_0$ is the yield stress, *k* is the porous parameter.

The equations governing of motion in the simplified form can be written as (lubrication approach)

$$Re\delta \left(u\frac{\partial}{\partial r} + w\frac{\partial}{\partial z}\right) w = -\frac{\partial p}{\partial z} + \frac{1}{r}\frac{\partial}{\partial r}(r\tau_{rz}) + \delta \frac{\partial}{\partial r}(\tau_{zz}) + \rho g sin\beta, \tag{10}$$

$$Re\delta^3 \left(u\frac{\partial}{\partial r} + w\frac{\partial}{\partial z}\right) u = -\frac{\partial p}{\partial r} + \frac{\delta}{r}\frac{\partial}{\partial r}(r\tau_{rr}) + \delta^2 \frac{\partial}{\partial r}(\tau_{rz}). \tag{11}$$

Using Long wavelength approximation ($\delta \ll 1$) and neglecting interia terms ($Re = 0$), above equations take the following form:

$$\frac{1}{r}\frac{\partial}{\partial r}(r\tau_{rz}) = -\frac{\partial p}{\partial z} + \frac{sin\beta}{F}, \tag{12}$$

$$\frac{\partial p}{\partial r} = 0, \tag{13}$$

where $\tau_{rz} = \mu\left(-\frac{\partial u}{\partial r}\right)^n + \tau_{0.}$ (14)

Here, τ_{rz} is the shear stress, *n* is the power law index and τ_0 is the yield stress.

The Eq. (12) is resolved using the boundary settings:

$$\psi = 0 \ \ at \ \ r = 0, \tag{15}$$

$$\frac{\partial}{\partial r}\left(\frac{1}{r}\frac{\partial \psi}{\partial r}\right) = 0 \ at \ \ r = 0, \tag{16}$$

$$\tau_{rz} = 0 \ \ at \ \ r = 0, \tag{17}$$

$$u = \ -\frac{\sqrt{Da}}{\alpha}\frac{\partial u}{\partial r} - 1 \quad at\ r = h = 1 + \frac{\lambda mz}{a_0} + \in \sin(2\pi z). \tag{18}$$

Here, u is velocity, α represents the slip constraint, Da: the Darcy number, and ϵ: the permeable node of the wall.

4. Solution of the Problem

Using $p = -\frac{\partial p}{\partial z}$ and $f = \frac{sin\beta}{F}$ in Eq. (12) we get $\frac{1}{r}\frac{\partial}{\partial r}(r\tau_{rz}) = p + f$ with Eq. (15) to Eq. (18), Further, Eq. (12) and Eq. (14) are designed for the velocity field:

$$u = \left(\frac{p+f}{2}\right)^k \left\{\frac{(t)^{k+1}}{k+1}\left[\left(\left(1 - \frac{s}{t}\right)^{k+1} - \left(\frac{r}{t} - \frac{s}{t}\right)^{k+1}\right)\right] + \frac{\sqrt{Da}}{\alpha}(r-s)^k\right\} - 1, \tag{19}$$

where $s = \frac{2\tau_{0.}}{p+f}$, $t = h - \in$.

Find the upper limit of the plug flow region by using the condition $\frac{\partial}{\partial r}\left(\frac{1}{r}\frac{\partial \psi}{\partial r}\right) = 0$ at $r = r_{0,}$ we have $r_0 = \frac{2\tau_0}{p+f}$, also by using condition $\tau_{rz} = \tau_h \ at \ r = \ h - \in$ we get $p + f = \frac{\tau_h}{h}$. Hence

$$\frac{r_0}{a} = \frac{\tau_0}{\tau_a} = \tau, \qquad 0 < \tau < 1, \tag{20}$$

Using Eq. (20) laterally with $r = r_0$ in Eq. (19), the plug movement speed is

$$u_p = \left(\frac{p+f}{2}\right)^k \frac{1}{k+1}\left\{(t)^{k+1}\left(1 - \frac{r_0}{t}\right)^{k+1}\right\} - 1 \quad for \quad 0 \le r \le r_0, \tag{21}$$

Integrate Eq. (19), Eq. (21) w. r. t r in addition, $\psi_p = 0 \ at \ r = 0$, $\psi = \psi_p \ at \ r = \ r_0$ we get the stream character as

$$\psi = \left(\frac{p+f}{2}\right)^k \left\{\frac{1}{k+1}\left[\left(\frac{r^2}{2}(H)^{k+1} - \frac{(R)^{k+2}(2r+rk+r_0)}{(k+2)(k+3)}\right)\right] + \frac{\sqrt{Da}}{\alpha}\frac{(R)^{k+1}(r+rk+r_0)}{(k+1)(k+2)}\right\} - \frac{r^2}{2}, \tag{22}$$

where $H = h-\epsilon -r_0$, $R = r - r_0$,

$$\psi_p = \int u_p \, dr = \left(\frac{p+f}{2}\right)^k \frac{1}{k+1}\{(H)^{k+1} - 1\}\frac{r^2}{2}. \quad (23)$$

The volume flux q through each cross-section in the wave frame is given by

$$q = 2\int_0^{r_0} u_p \, r dr + 2\int_{r_0}^{h-\epsilon} u \, r dr$$

$$= \left(\frac{p+f}{2}\right)^k \frac{(h-\epsilon)^{k+3}}{k+1}\left(1 - \frac{r_0}{h-\epsilon}\right)^{k+1}\left[1 - \frac{2\left(1-\frac{r_0}{h-\epsilon}\right)(k+2+\frac{r_0}{h-\epsilon})}{(k+2)(k+3)} + 2\frac{\sqrt{Da}}{\alpha(h-\epsilon)}\left(1 + k + \frac{r_0}{h-\epsilon}\right)\right] - (h-\epsilon)^2. \quad (24)$$

The instant dimensions flow rate $Q(X,t)$ in the research laboratory borders between the fundamental line and the partition is

$$Q(X,t) = 2\int_0^{h-\epsilon}(w+1)r \, dr = \left(\frac{p+f}{2}\right)^k \frac{(h-\epsilon)^{k+3}}{k+1}\left(1 - \frac{r_0}{h-\epsilon}\right)^{k+1} \times \left[1 - \frac{2\left(1-\frac{r_0}{h-\epsilon}\right)(k+2+\frac{r_0}{h-\epsilon})}{(k+2)(k+3)} + 2\frac{\sqrt{Da}}{\alpha(h-\epsilon)}\left(1 + k + \frac{r_0}{h-\epsilon}\right)\right]$$

From Eq. (24) we take

$$\frac{dp}{dz} = \frac{-2\left(q+(h-\epsilon)^2\right)^{\frac{1}{k}}(k+1)^{\frac{1}{k}}}{(h-\epsilon)^{1+\frac{3}{k}}\left(1-\frac{r_0}{h-\epsilon}\right)^{1+\frac{1}{k}}\left[1-\frac{2\left(1-\frac{r_0}{h-\epsilon}\right)(k+2+\frac{r_0}{h-\epsilon})}{(k+2)(k+3)}+2\frac{\sqrt{Da}}{\alpha(h-\epsilon)}\left(1+k+\frac{r_0}{h-\epsilon}\right)\right]^{\frac{1}{k}}} + f. \quad (25)$$

Averaging the Eq. (24) over single time period produces the period mean flow (time averaged volume flow rate) $\bar{Q}$ as

$$\bar{Q} = \int_0^T \int_0^{(h-\epsilon)}(w+1)r \, dr \, dt = q + \frac{1}{T}\int_0^T (h-\epsilon)^2 \, dt = q + 1 + \frac{\phi^2}{2}. \quad (26)$$

Integrating the Eq. (25) w r t 'z' one wave length, the pressure drops over a single cycle of the wave

$$\Delta p = \int_0^1 \frac{-2\left[\bar{Q}-1-\frac{\phi^2}{2}+(h-\epsilon)^2\,(k+1)\right]^{\frac{1}{k}}}{(h-\epsilon)^{1+\frac{3}{k}}\left(1-\frac{r_0}{h-\epsilon}\right)^{1+\frac{1}{k}}\left[1-\frac{2\left(1-\frac{r_0}{h-\epsilon}\right)(k+2+\frac{r_0}{h-\epsilon})}{(k+2)(k+3)}+2\frac{\sqrt{Da}}{\alpha(h-\epsilon)}\left(1+k+\frac{r_0}{h-\epsilon}\right)\right]^{\frac{1}{k}}} dz + f \, . \quad (27)$$

The dimensionless frictional power F at the wall diagonal single wavelength of the tube is assumed by

$$F = \int_0^1 (h-\epsilon)^2\left(-\frac{dp}{dz}\right)dz$$

$$= \int_0^1 \frac{2(h-\epsilon)^2\left[\left(\bar{Q}-1-\frac{\phi^2}{2}+(h-\epsilon)^2\right)(k+1)\right]^{\frac{1}{k}}}{(h-\epsilon)^{1+\frac{3}{k}}\left(1-\frac{r_0}{h-\epsilon}\right)^{1+\frac{1}{k}}\left[1-\frac{2\left(1-\frac{r_0}{h-\epsilon}\right)(k+2+\frac{r_0}{h-\epsilon})}{(k+2)(k+3)}+2\frac{\sqrt{Da}}{\alpha(h-\epsilon)}\left(1+k+\frac{r_0}{h-\epsilon}\right)\right]^{\frac{1}{k}}} dz + f \, . \quad (28)$$

5. Results and Discussion

The pressure difference Δp is calculated as a function of $\bar{Q}$ from Eq. (14) and variation of different parameters are observed for fixed values of $n, Da, \alpha, \epsilon, r_0, l, a, F, \beta$ and are shown in Figure 2 to Figure 9.

The variation of Darcy number *Da* for change in the inclination of the tube β is shown in Figure 2 and Figure 3 and is noticed that smaller the Darcy number, the greater the pressure rise in contrast to how the pump works. In the free pumping region, no change is observed in flux $\bar{Q}$ for variation in Darcy number. The results are comparable with the results of Prasad *et al.,* [17]. The effect of changing values of α, with different inclination angles β are depicted in Figure 4 and Figure 5. In the pumping region, increased slip parameters reduce friction between the fluid and the channel walls, facilitating the fluid flow and causing a higher pressure difference. Conversely, in the co-pumping region, where both the fluid and walls move in the same direction, increased slip reduces the relative motion resistance, lowering the pressure difference due to the decreased energy required to maintain flow.

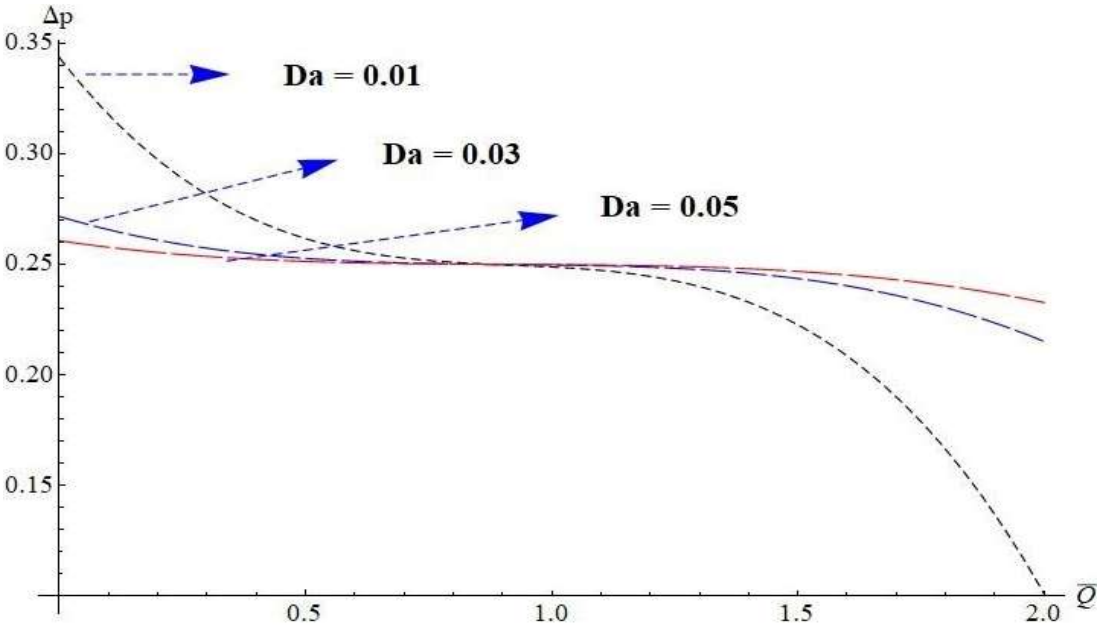

Fig. 2. Outcomes of Darcy parameter. For fix values $n = 3, \alpha = 0.1, \epsilon = 0.01, r_0 = 0.2, l = 0.3, a = 0.2, F = 2, \beta = \frac{\pi}{6}$

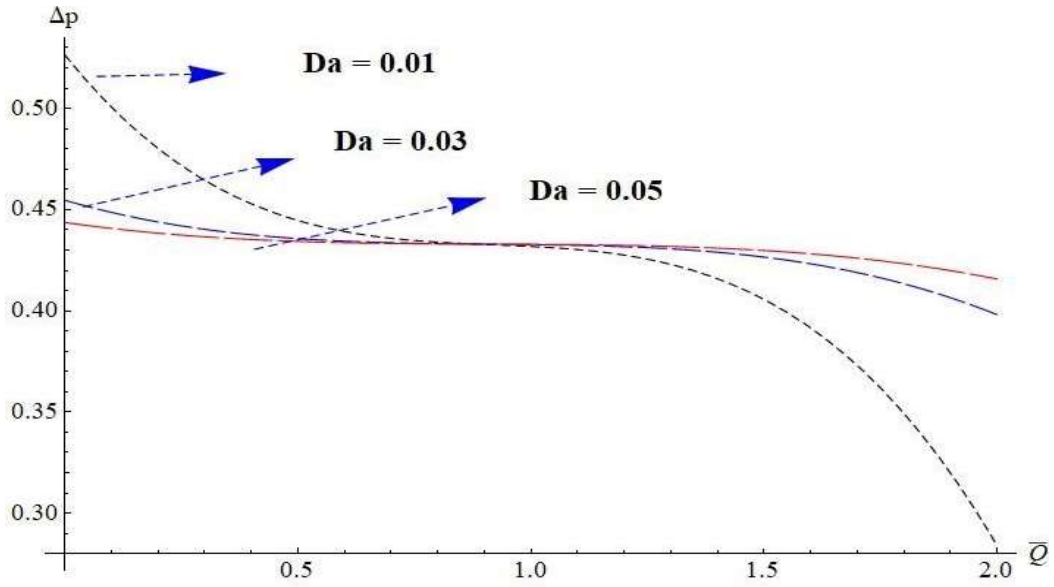

Fig. 3. Results of Darcy parameter. For fix values $n = 3, \alpha = 0.1, \epsilon = 0.01, r_0 = 0.2, l = 0.3, a = 0.2, F = 2, \beta = \frac{\pi}{3}$

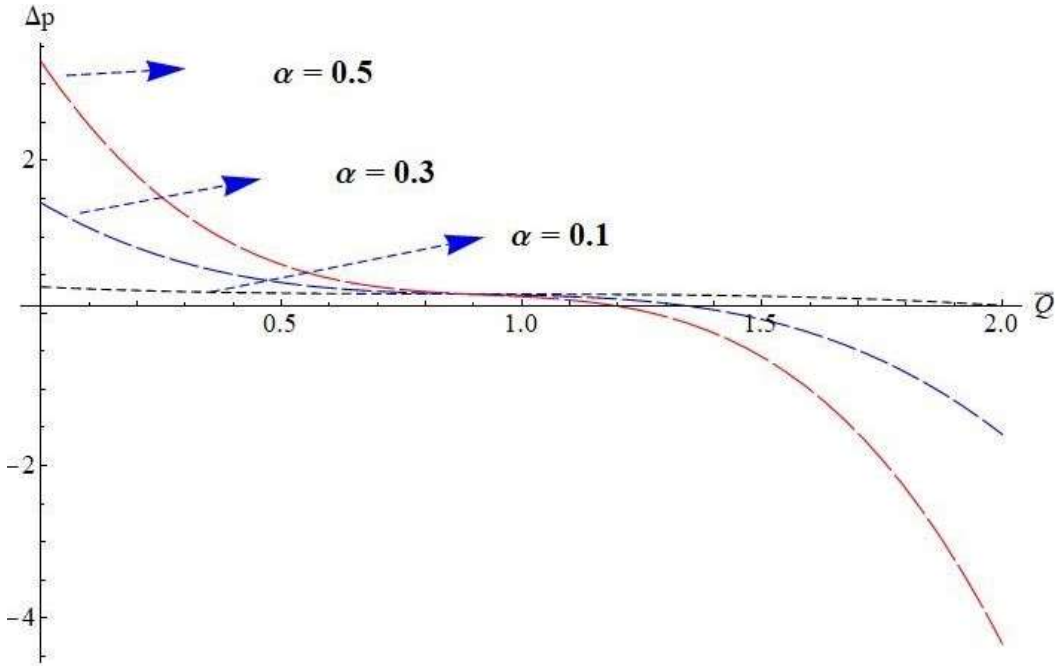

Fig. 4. Results of slip parameter. For fix values $Da = 0.01, \epsilon = 0.01, n = 3, r_0 = 0.2, l = 0.3, a = 0.2, F = 2, \beta = \frac{\pi}{6}$

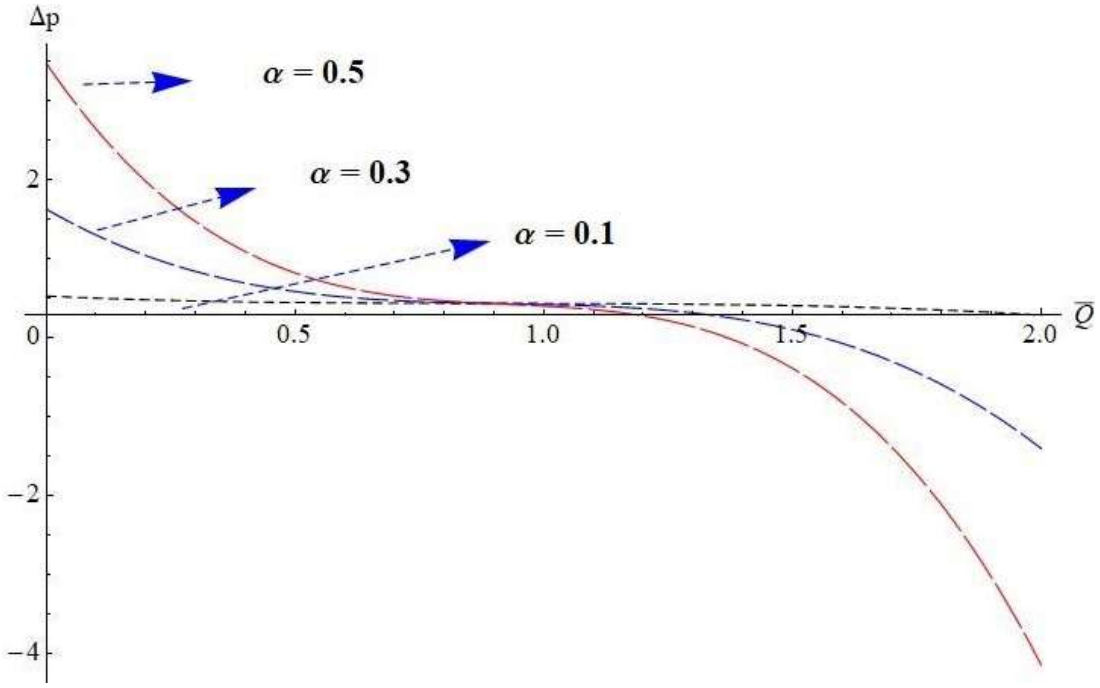

Fig. 5. Results of slip parameter. For fix values $Da = 0.01, \epsilon = 0.01, n = 3, r_0 = 0.2, l = 0.3, a = 0.2, F = 2, \beta = \frac{\pi}{3}$

To observe the impacts of varying the porous thickening of the channel wall, Figure 6 and Figure 7 are drawn. They emphasize the positive impact of the porous thickening on the pressure difference in the pumping region. To understand the behavior of pressure rise under the effect of the power law index parameter, different angular inclination Figure 8 and Figure 9 are put forth. The graphs reveal the decrease in pressure rise with an increase in the power law index in the pumping region, and opposite behavior is seen in the co-pumping region. Physically as the power law index increases, the fluid becomes more shear-thinning. This reduces the viscous resistance, allowing the fluid to move more easily, resulting in a lower pressure rise for the same flow rate. They are also in agreement with the results of Prasad *et al.,* [17].

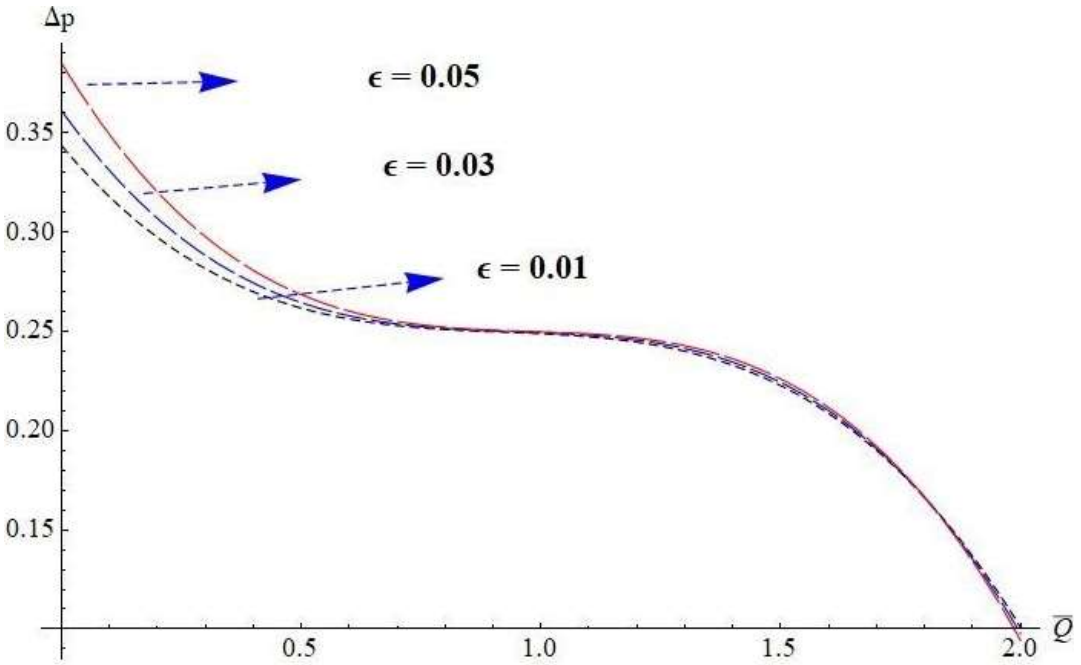

Fig. 6. Results of porous thickening of the wall. $Da = 0.01, \alpha = 0.1, n = 3, r_0 = 0.2, l = 0.3, a = 0.2, F = 2, \beta = \frac{\pi}{6}$

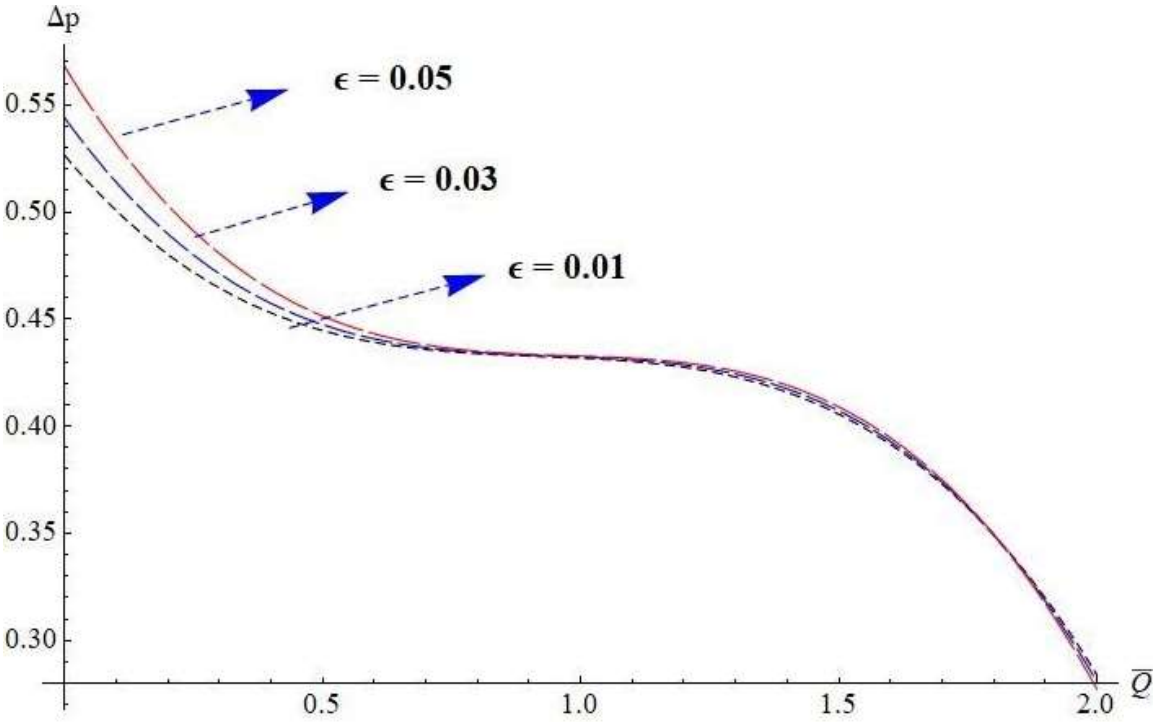

Fig. 7. Results of porous thickening of the wall. $Da = 0.01, , \alpha = 0.1, n = 3, r_0 = 0.2, l = 0.3, a = 0.2, F = 2, \beta = \frac{\pi}{3}$

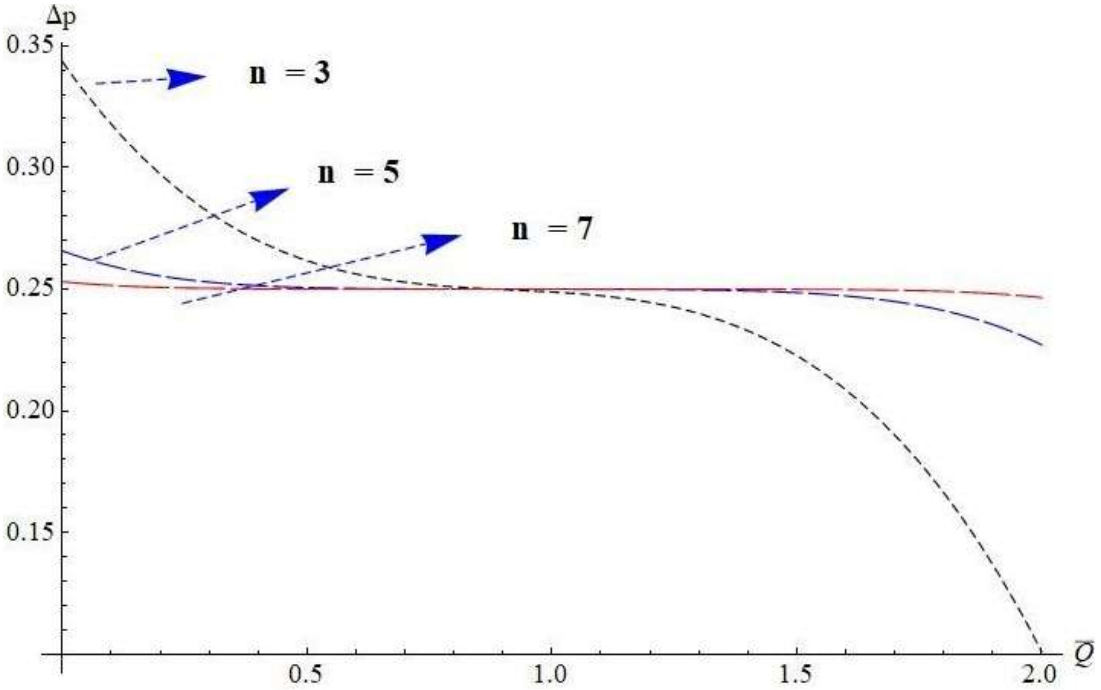

Fig. 8. Results of power law index. $Da = 0.01,, \alpha = 0.1, \epsilon = 0.01, r_0 = 0.2, l = 0.3, a = 0.2, F = 2\,, \beta = \frac{\pi}{6}$

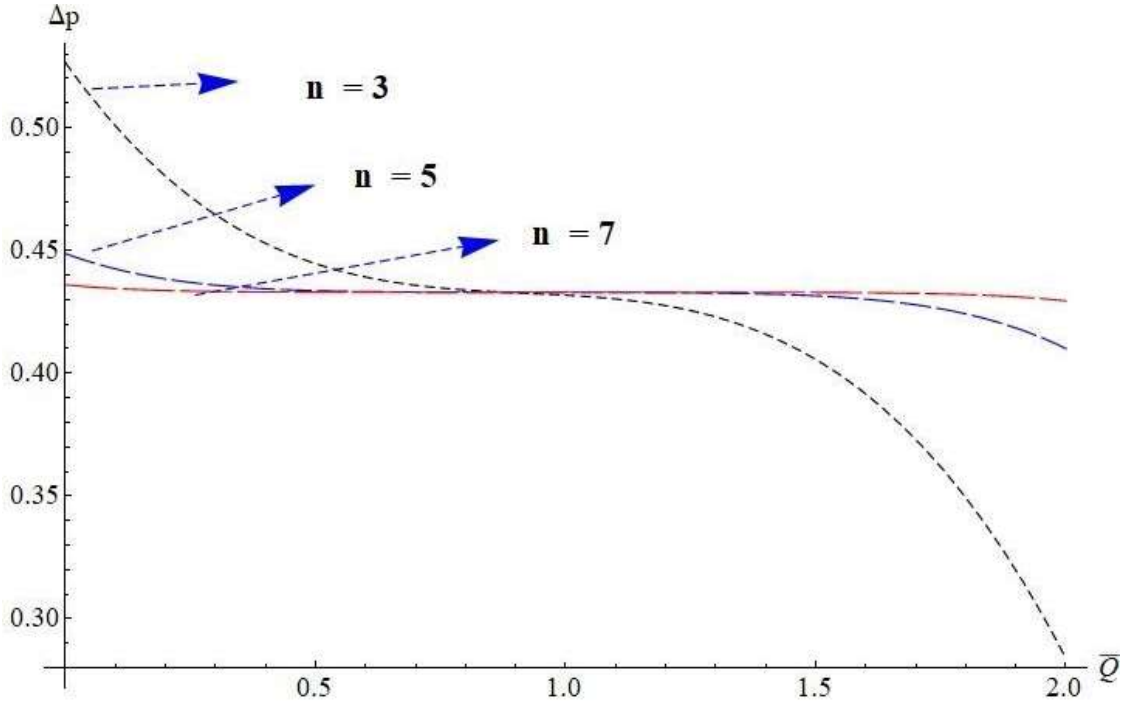

Fig. 9. Results of power law index. $Da = 0.01,, \alpha = 0.1, \epsilon = 0.01, r_0 = 0.2, l = 0.3, a = 0.2, F = 2, \beta = \frac{\pi}{3}$

A graphic depiction of the variation of the time-averaged volume flow rate $\bar{Q}$ with frictional force F is exhibited in the Figure 10 to Figure 17, using Eq. (18). Assuming fixed values, of $\alpha\,, \epsilon, r_0\,, l, a\,, F\,, n$ the behavior of parameters of interest is analyzed by taking two different inclination angles ($\beta = \frac{\pi}{6}\ and\ \frac{\pi}{3}$).

Figure 10 and Figure 11 show a reduction in pressure rise with an increase in the Darcy number as the inclination increases. Physically, it indicates that both higher permeability (Darcy number) and greater inclination reduce the resistance to flow, decreasing the pressure required for the fluid movement. The results are in agreement with those of Sankad and Patil [18]. With a rise in the inclination angle, the slip parameter exhibits a positive impact on the pressure rise, as shown in Figure 12 and Figure 13, whereas the porous thickening of the wall shows a negative impact. As illustrated in Figure 14 and Figure 15. Observing the Figure 16 and Figure 17, it is accepted that the power law index decreases the pressure rise, and the result is seen to agree with the result of Sankad and Patil [18].

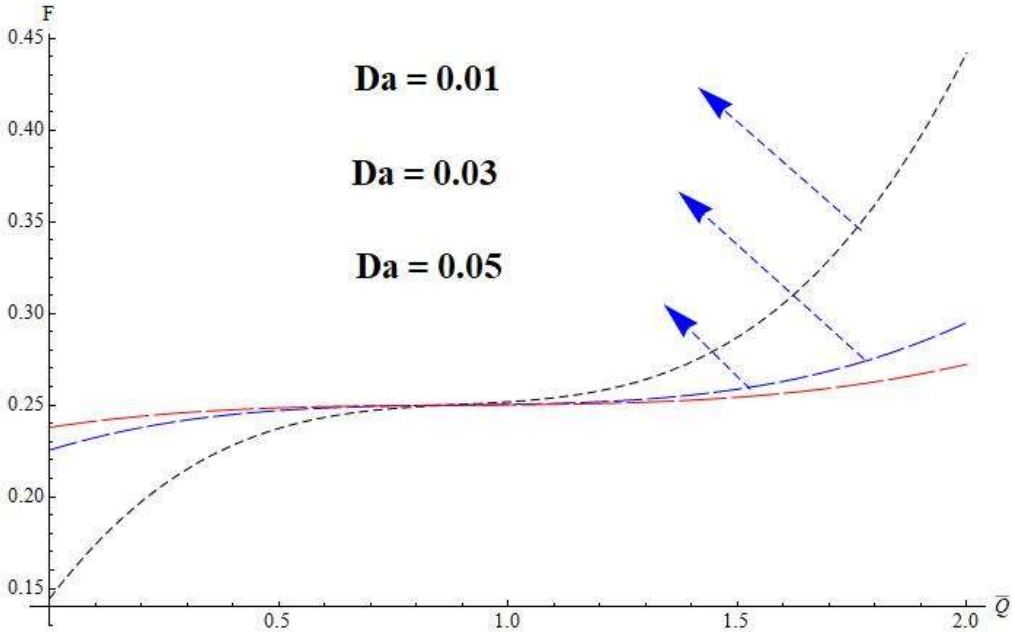

Fig. 10. Results of Darcy parameter. $n = 3, \alpha = 0.1, \epsilon = 0.01, r_0 = 0.2, l = 0.3, a = 0.2, F = 2, \beta = \frac{\pi}{6}$

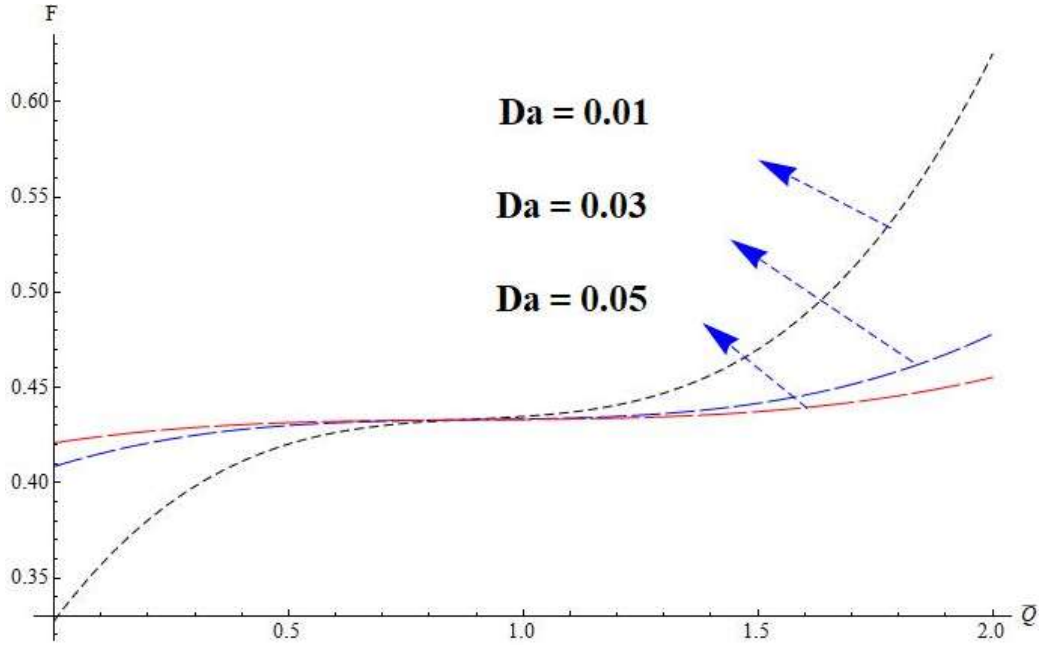

Fig. 11. Results of Darcy parameter. $n = 3, \alpha = 0.1, \epsilon = 0.01, r_0 = 0.2, l = 0.3, a = 0.2, F = 2, \beta = \frac{\pi}{3}$

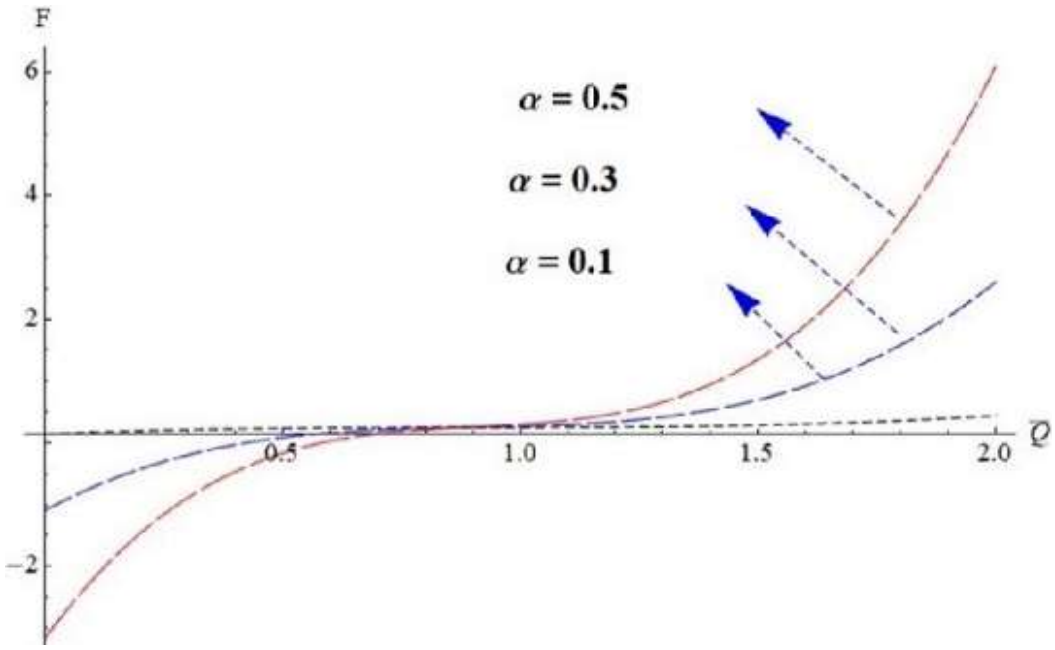

Fig. 12. Results of slip parameter. $Da = 0.01, \epsilon = 0.01, n = 3, r_0 = 0.2, l = 0.3, a = 0.2, F = 2, \beta = \frac{\pi}{6}$

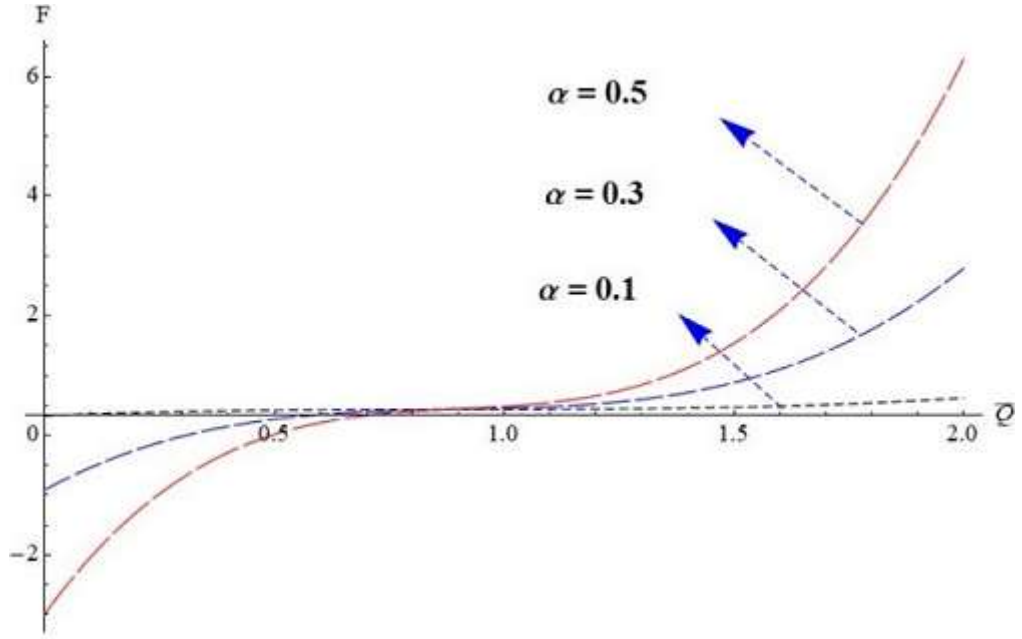

Fig. 13. Results of slip parameter. $Da = 0.01, \epsilon = 0.01, n = 3, r_0 = 0.2, l = 0.3, a = 0.2, F = 2, \beta = \frac{\pi}{3}$

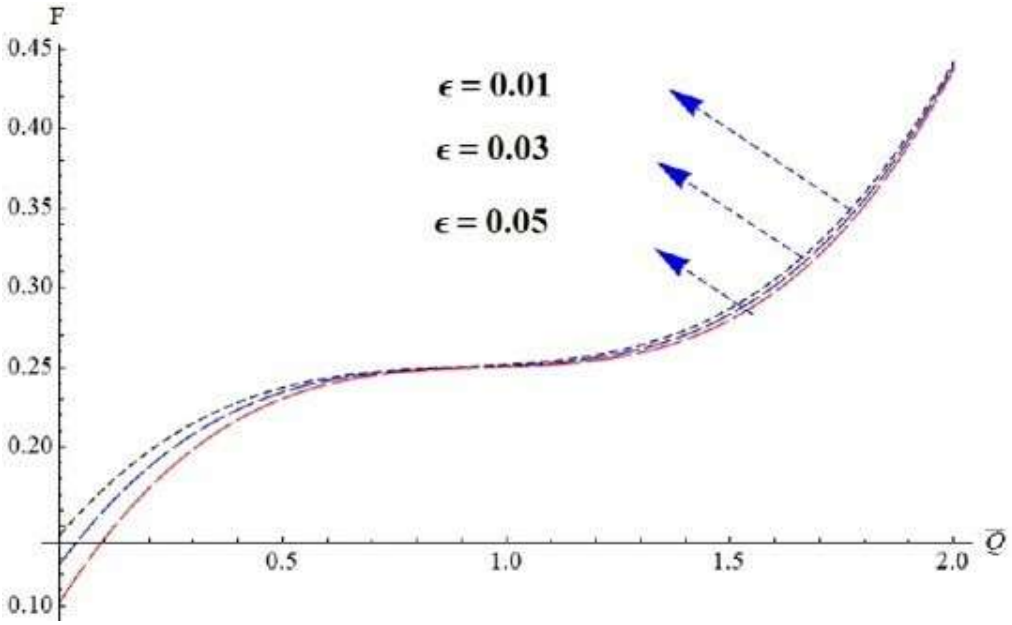

Fig. 14. Results of porous thickening of the wall. $Da = 0.01, \alpha = 0.1, n = 3, r_0 = 0.2, l = 0.3, a = 0.2, F = 2, \beta = \frac{\pi}{6}$

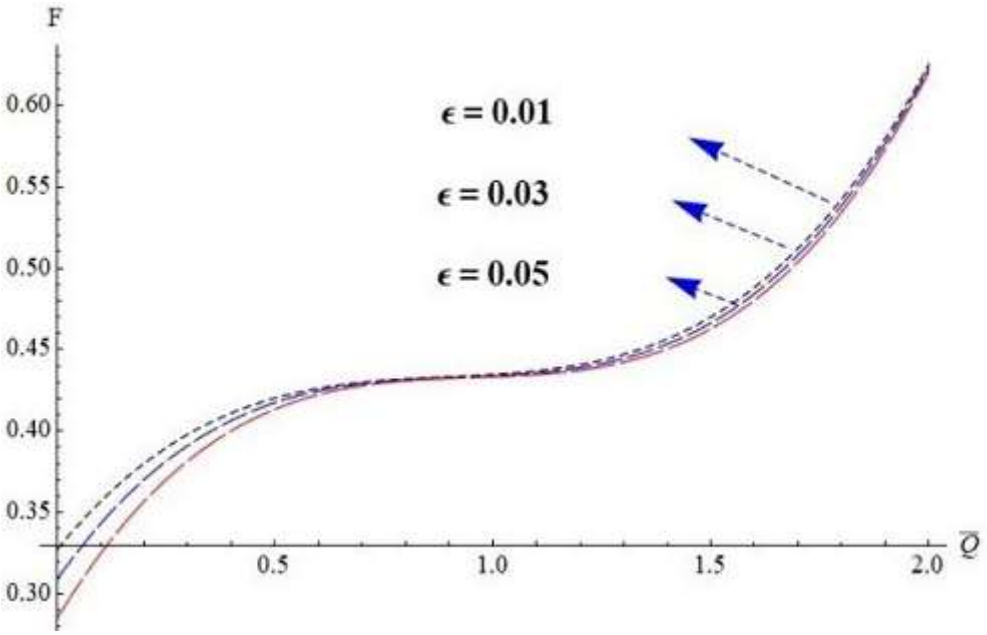

Fig. 15. Results of porous thickening of the wall. $Da = 0.01, \alpha = 0.1,\ n = 3, r_0 = 0.2, l = 0.3, a = 0.2, F = 2, \beta = \frac{\pi}{3}$

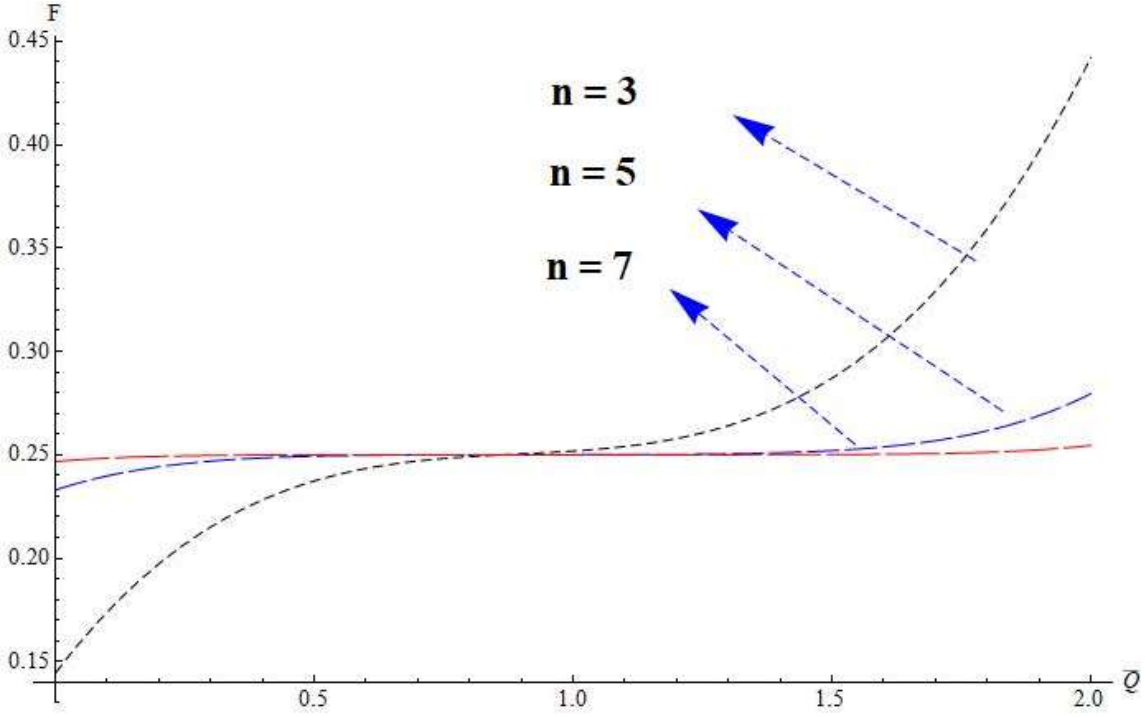

Fig. 16. Results of power law index. $Da = 0.01, , \alpha = 0.1, \epsilon = 0.01, r_0 = 0.2, l = 0.3, a = 0.2, F = 2\ , \beta = \frac{\pi}{6}$

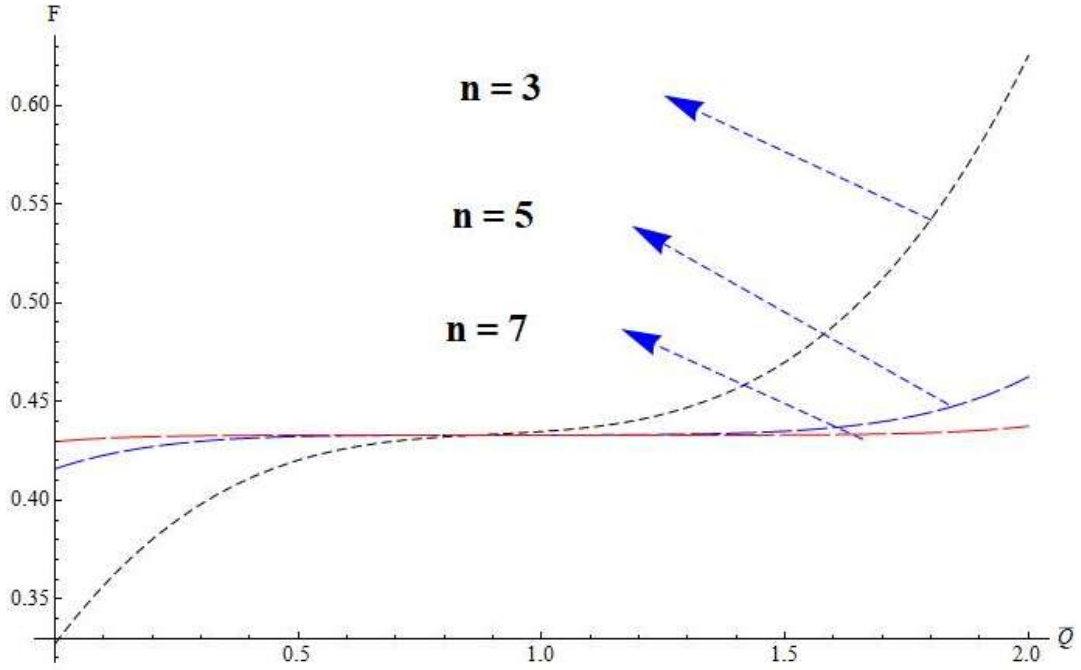

Fig. 17. Results of power law index. $Da = 0.01,, \alpha = 0.1, \epsilon = 0.01, r_0 = 0.2, l = 0.3, a = 0.2, F = 2, \beta = \frac{\pi}{3}$

Trapping phenomenon is one of the important mechanisms found in the human body in the transportation of food bolus through the esophagus. This phenomenon is observed pictorially in Figure 18 to Figure 27. Figure 18 and Figure 19 exhibited that the increase in the size of the bolus with an increase in the Darcy number means that as the permeability of the porous medium increases, fluid can flow more freely, causing larger bolus formations. The enhancement of bolus size with the slip parameter indicates that reduced friction at the boundaries also facilitates the movement of fluid, allowing larger boluses to form. Physically, both higher permeability and reduced boundary friction contribute to the ease of fluid movement, leading to larger trapped fluid regions, as observed in Figure 20 and Figure 21. The size of the bolus increases with a rise in the values of porous thickening of the wall, as can be seen from Figure 22 and Figure 23. An Increase in the power law index reduces the size of the trapped bolus, as depicted in Figure 24 and Figure 25. The trapping phenomenon observed for varying the inclination clarifies that the bolus condenses and is pictorially shown in Figure 26 and Figure 27.

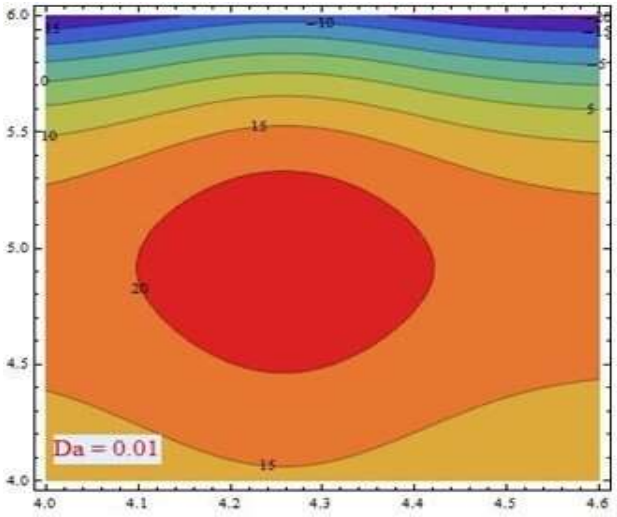

Fig. 18. $Da = 0.01, \epsilon = 0.6, r_0 = 0.02, \beta = \pi/4\,, l = 0.2, F = 2, p = 0.8, n = 0.3$

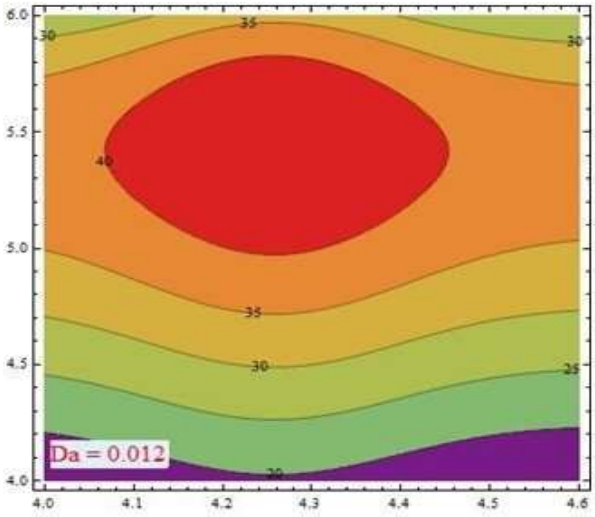

Fig. 19. $Da = 0.01, \epsilon = 0.6, r_0 = 0.02, \beta = \pi/4\,, l = 0.2, F = 2, p = 0.8, n = 0.3$

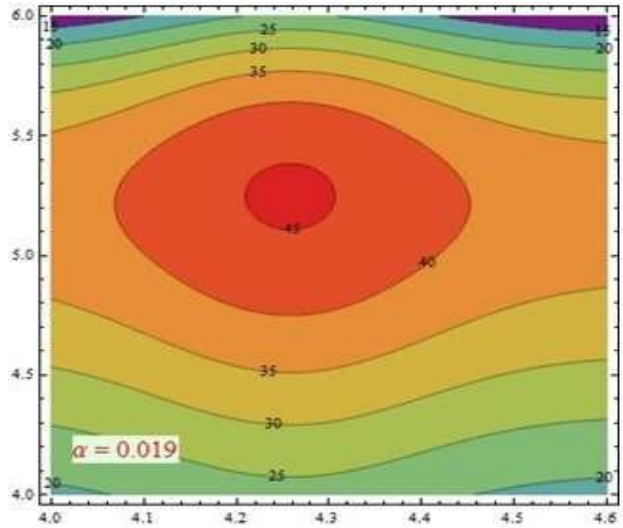

Fig. 20. $Da = 0.01, \epsilon = 0.6, r_0 = 0.02, \beta = \pi/4\,, l = 0.2, F = 2, p = 0.8, n = 0.3$

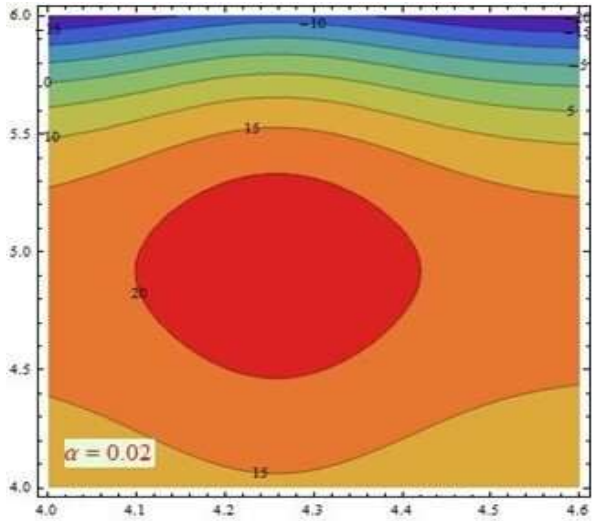

Fig. 21. $Da = 0.01, \epsilon = 0.6, r_0 = 0.02, \beta = \pi/4\,, l = 0.2, F = 2, p = 0.8, n = 0.3$

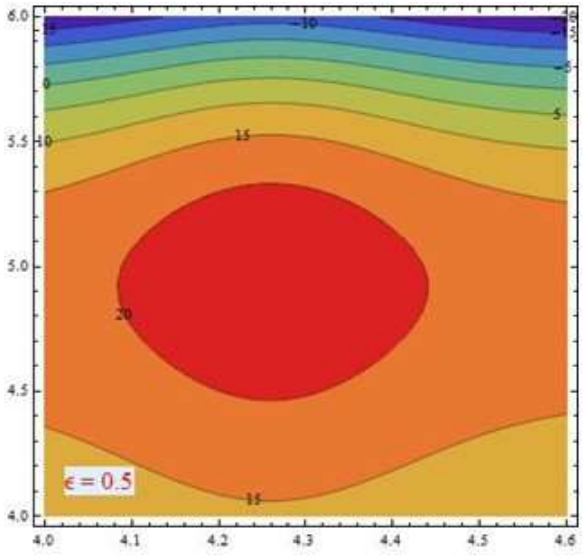

Fig. 22. $Da = 0.01, \alpha = 0.02, r_0 = 0.02, \beta = \pi/4\,, l = 0.2, F = 2, p = 0.8, n = 0.3$

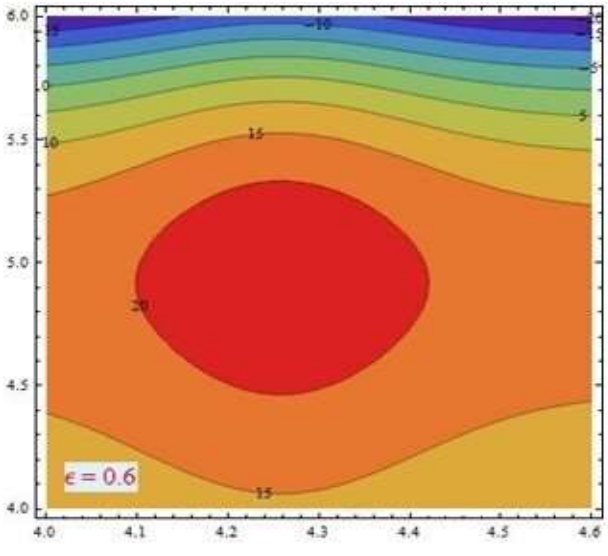

Fig. 23. $Da = 0.01, \alpha = 0.02, r_0 = 0.02, \beta = \pi/4\,, l = 0.2, F = 2, p = 0.8, n = 0.3$

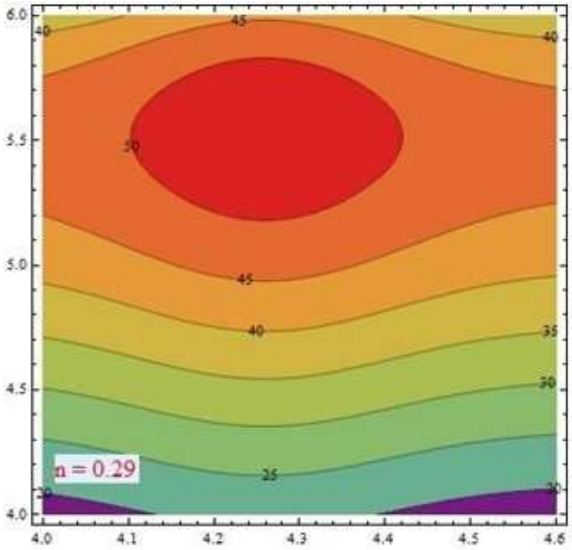

Fig. 24. $Da = 0.01, \alpha = 0.02, \epsilon = 0.6, r_0 = 0.02, \beta = \pi/4\,, l = 0.2, F = 2, p = 0.8$

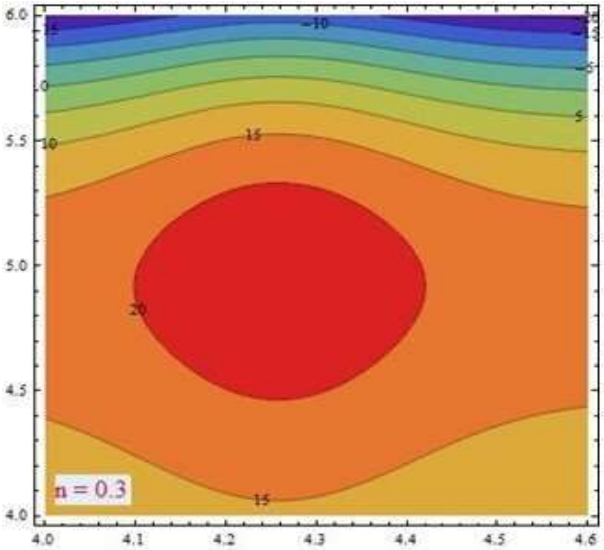

Fig. 25. $Da = 0.01, \alpha = 0.02, \epsilon = 0.6, r_0 = 0.02, \beta = \pi/4\,, l = 0.2, F = 2, p = 0.8$

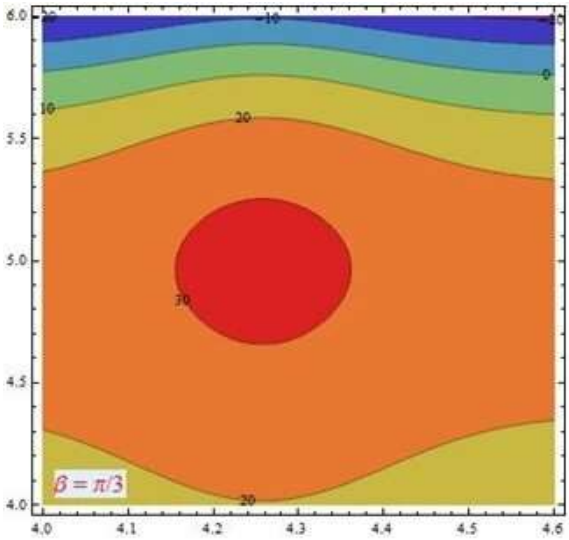

Fig. 26. $Da = 0.01, \alpha = 0.02, \epsilon = 0.6, r_0 = 0.02, l = 0.2, F = 2, p = 0.8, n = 0.3$

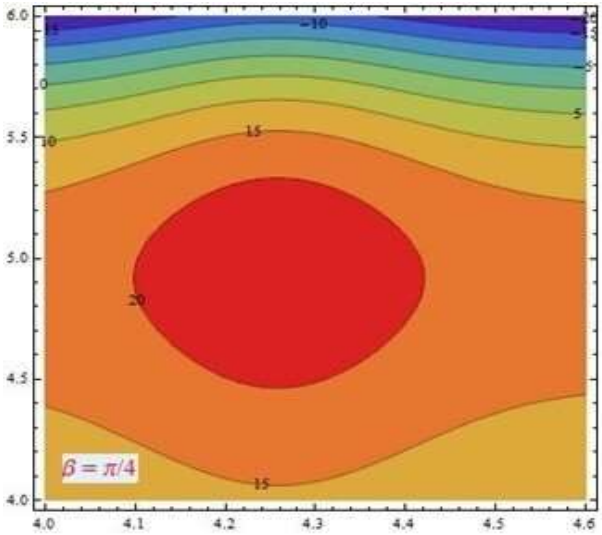

Fig. 27. $Da = 0.01, \alpha = 0.02, \epsilon = 0.6, r_0 = 0.02, l = 0.2, F = 2, p = 0.8, n = 0.3$

6. Conclusion

In this study, the Herschel-Bulkley fluid model was evaluated for the passage induced by sinusoidal peristaltic waves with a small Reynolds number through non-uniform inclined tube. These formulas were analyzed both analytically and numerically using MATHEMATICA software, and the key findings regarding the main flow issues are summarized below.

i. A smaller Darcy number indicates lower permeability of the porous medium, which restricts fluid flow and requires a higher pressure rise to drive the fluid through. This behavior contrasts with typical pump operation, where higher permeability (larger Darcy number) would generally result in a lower pressure rise needed for the same flow rate. Essentially, in systems with low Darcy numbers, more pressure is required to overcome the resistance posed by the less permeable medium
ii. Pressure drops increase with the porous thickening of the wall and slip parameter, but decrease with power law index and Darcy number.
iii. A reduction in pressure rise with an increase in the Darcy number as the inclination increases. Physically, it indicates that both higher permeability (Darcy number) and greater inclination reduce the resistance to flow, decreasing the pressure required for the fluid movement.
iv. When the wall's porous thickening values increase, it implies the wall's permeability is enhanced, allowing more fluid to pass through it. This facilitates the accumulation of fluid in certain regions, resulting in larger boluses. Essentially, higher porous thickening reduces resistance to fluid flow, allowing more fluid to be trapped and form larger boluses.

Acknowledgement
This research was not funded by any grant.

References

[1] Latham, Thomas Walker. "Fluid motions in a peristaltic pump." *PhD diss., Massachusetts Institute of Technology*, 1966.
[2] Gupta, B. B., and V. Seshadri. "Peristaltic pumping in non-uniform tubes." *Journal of Biomechanics* 9, no. 2 (1976): 105-109. https://doi.org/10.1016/0021-9290(76)90130-5

[3] Misra, J. C., and S. K. Pandey. "Peristaltic transport of blood in small vessels: study of a mathematical model." *Computers & Mathematics with Applications* 43, no. 8-9 (2002): 1183-1193. https://doi.org/10.1016/S0898-1221(02)80022-0
[4] Srinivasacharya, D., M. Mishra, and A. Ramachandra Rao. "Peristaltic pumping of a micropolar fluid in a tube." *Acta Mechanica* 161 (2003): 165-178. https://doi.org/10.1007/s00707-002-0993-y
[5] Rani, P. Naga, and G. Sarojamma. "Peristaltic transport of a Casson fluid in an asymmetric channel." *Australasian Physical and Engineering Sciences in Medicine* 27, no. 2 (2004): 49-59. https://doi.org/10.1007/BF03178376
[6] Rao, A. Ramachandra, and Manoranjan Mishra. "Peristaltic transport of a power-law fluid in a porous tube." *Journal of Non-Newtonian Fluid Mechanics* 121, no. 2-3 (2004): 163-174. https://doi.org/10.1016/j.jnnfm.2004.06.006
[7] Reddy, M. Gnaneswara. "Heat and mass transfer on magnetohydrodynamic peristaltic flow in a porous medium with partial slip." *Alexandria Engineering Journal* 55, no. 2 (2016): 1225-1234. https://doi.org/10.1016/j.aej.2016.04.009
[8] Nadeem, S., and Noreen Sher Akbar. "Influence of heat transfer on a peristaltic transport of Herschel-Bulkley fluid in a non-uniform inclined tube." *Communications in Nonlinear Science and Numerical Simulation* 14, no. 12 (2009): 4100-4113. https://doi.org/10.1016/j.cnsns.2009.02.032
[9] Maiti, Somnath, and J. C. Misra. "Non-Newtonian characteristics of peristaltic flow of blood in micro-vessels." *Communications in Nonlinear Science and Numerical Simulation* 18, no. 8 (2013): 1970-1988. https://doi.org/10.1016/j.cnsns.2012.12.015
[10] Sankad, G. C., and Asha Patil. "Effect of Porosity on the Peristaltic Pumping of a NonNewtonian Fluid in a Channel." *Journal of New Results in Science* 5, no. 10 (2016): 1-9.
[11] Vajravelu, K., S. Sreenadh, and V. Ramesh Babu. "Peristaltic pumping of a Herschel-Bulkley fluid in a channel." *Applied Mathematics and Computation* 169, no. 1 (2005): 726-735. https://doi.org/10.1016/j.amc.2004.09.063
[12] Vajravelu, K., S. Sreenadh, and V. Ramesh Babu. "Peristaltic transport of a Herschel-Bulkley fluid in an inclined tube." *International Journal of Non-Linear Mechanics* 40, no. 1 (2005): 83-90. https://doi.org/10.1016/j.ijnonlinmec.2004.07.001
[13] Vajravelu, K., S. Sreenadh, and V. Babu. "Peristaltic transport of a Herschel-Bulkley fluid in contact with a Newtonian fluid." *Quarterly of Applied Mathematics* 64, no. 4 (2006): 593-604. https://doi.org/10.1090/S0033-569X-06-01020-9
[14] Selvi, C. K., and A. N. S. Srinivas. "Peristaltic transport of Herschel-Bulkley fluid in a non-uniform elastic tube." *Propulsion and Power Research* 8, no. 3 (2019): 253-262. https://doi.org/10.1016/j.jppr.2018.07.010
[15] Pandey, S. K., and Dharmendra Tripathi. "Influence of magnetic field on the peristaltic flow of a viscous fluid through a finite-length cylindrical tube." *Applied Bionics and Biomechanics* 7, no. 3 (2010): 169-176. https://doi.org/10.1155/2010/294517
[16] Takagi, D., and N. J. Balmforth. "Peristaltic pumping of viscous fluid in an elastic tube." *Journal of Fluid Mechanics* 672 (2011): 196-218. https://doi.org/10.1017/S0022112010005914
[17] Prasad, K. Maruthi, N. Subadra, and M. A. S. Srinivas. "Peristaltic transport of a nanofluid in an inclined tube." *American Journal of Computational and Applied Mathematics* 5, no. 4 (2015): 117-128.
[18] Sankad, G. C., and Asha Patil. "Impact of permeable lining of the wall on the peristaltic flow of Herschel Bulkley fluid." *Applications and Applied Mathematics: An International Journal (AAM)* 11, no. 2 (2016): 663-679.
[19] Kavitha, A., R. Hemadri Reddy, R. Saravana, and S. Sreenadh. "Peristaltic transport of a Jeffrey fluid in contact with a Newtonian fluid in an inclined channel." *Ain Shams Engineering Journal* 8, no. 4 (2017): 683-687. https://doi.org/10.1016/j.asej.2015.10.014
[20] Vaidya, Hanumesh. "Influence of velocity slip and heat transfer on peristaltic transport of Jeffery fluid in an inclined elastic tube." *International Journal of Creative Research Thoughts (IJCRT)* 5, no. 2 (2017): 288-302.
[21] Gudekote, Manjunatha, and Rajashekhar Choudhari. "Slip effects on peristaltic transport of Casson fluid in an inclined elastic tube with porous walls." *Journal of Advanced Research in Fluid Mechanics and Thermal Sciences* 43, no. 1 (2018): 67-80.
[22] Devaki, P., A. Kavitha, D. Venkateswarlu Naidu, and S. Sreenadh. "The influence of wall properties on the peristaltic pumping of a casson fluid." In *Applied Mathematics and Scientific Computing: International Conference on Advances in Mathematical Sciences*, Vellore, India, December 2017-Volume II, pp. 167-179. Springer International Publishing, 2019. https://doi.org/10.1007/978-3-030-01123-9_18
[23] Vaidya, Hanumesh, Oluwole Daniel Makinde, Rajashekhar Choudhari, Kerehalli Vinayaka Prasad, Sami Ullah Khan, and Kuppalapalle Vajravelu. "Peristaltic flow of non-Newtonian fluid through an inclined complaint nonlinear tube: application to chyme transport in the gastrointestinal tract." *The European Physical Journal Plus* 135, no. 11 (2020): 1-15. https://doi.org/10.1140/epjp/s13360-020-00899-3

[24] Ramachandran, Saravana, Kuppalapalle Vajravelu, K. V. Prasad, and S. Sreenadh. "Peristaltic-ciliary flow of a Casson fluid through an inclined tube." *Communication in Biomathematical Sciences* 4, no. 1 (2021): 23-38. https://doi.org/10.5614/cbms.2021.4.1.3

[25] Devakar, M., K. Ramesh, and K. Vajravelu. "Magnetohydrodynamic effects on the peristaltic flow of couple stress fluid in an inclined tube with endoscope." *Journal of Computational Mathematics and Data Science* 2 (2022): 100025. https://doi.org/10.1016/j.jcmds.2022.100025

[26] Abbas, Z., A. Shakeel, M. Y. Rafiq, S. Khaliq, J. Hasnain, and A. Nadeem. "Rheology of peristaltic flow in couple stress fluid in an inclined tube: Heat and mass transfer analysis." *Advances in Mechanical Engineering* 14, no. 11 (2022): 16878132221139984. https://doi.org/10.1177/16878132221139984

[27] Kotnurkar, Asha S., and Vijaylaxmi T. Talawar. "Influence of thermal jump and inclined magnetic field on peristaltic transport of Jeffrey fluid with silver nanoparticle in the eccentric annulus." *Heliyon* 8, no. 9 (2022). https://doi.org/10.1016/j.heliyon.2022.e10543

[28] Moatimid, Galal M., Mona A. A. Mohamed, and Khaled Elagamy. "Peristaltic transport of Rabinowitsch nanofluid with moving microorganisms." *Scientific Reports* 13, no. 1 (2023): 1863. https://doi.org/10.1038/s41598-023-28967-5

[29] Ali, Shahbaz, Sohail Nadeem, Nevzat Akkurt, Hassan Ali Ghazwani, and Sayed M. Eldin. "Numerical simulation for peristalsis of Quemada fluid: A dynamic mesh approach." *Journal of Advanced Research* 54 (2023): 77-88. https://doi.org/10.1016/j.jare.2023.01.022

[30] Abuiyada, Alaa, Nabil Eldabe, Mohamed Abouzeid, and Samy Elshaboury. "Influence of both Ohmic dissipation and activation energy on peristaltic transport of Jeffery nanofluid through a porous media." *CFD Letters* 15, no. 6 (2023): 65-85. https://doi.org/10.37934/cfdl.15.6.6585